Correction to "Scattering by a Lossy Dielectric Circular Cylindrical Multilayer, Numerical Values"

Salvatore Caorsi and Matteo Pastorino

In implementing the Richmond method for the computation of the scattering by multilayer lossy dielectric cylinders, we found an error in the above paper.[1] More precisely, the elements of the recursive equation (4) (obtained by enforcing the continuity conditions at the boundary between each pair of concentric cylinders) should be rectified as follows

$$U_{mn} = \xi^{-1}[\mu_m k_{m+1} J_n(k_m r_m) Y_n'(k_{m+1} r_m) - \mu_{m+1} k_m J_n'(k_m r_m) Y_n(k_{m+1} r_m)] \quad (5a)$$

$$V_{mn} = \xi^{-1}[\mu_{m+1} k_m J_n(k_{m+1} r_m) J_n'(k_m r_m) - \mu_m k_{m+1} J_n'(k_{m+1} r_m) J_n(k_m r_m)] \quad (5b)$$

$$W_{mn} = \xi^{-1}[\mu_m k_{m+1} Y_n(k_m r_m) Y_n'(k_{m+1} r_m) - \mu_{m+1} k_m Y_n'(k_m r_m) Y_n(k_{m+1} r_m)] \quad (5c)$$

$$X_{mn} = \xi^{-1}[\mu_{m+1} k_m Y_n'(k_m r_m) J_n(k_{m+1} r_m) - \mu_m k_{m+1} Y_n(k_m r_m) J_n'(k_{m+1} r_m)] \quad (5d)$$

$$\xi = \mu_m k_{m+1}[Y_n'(k_{m+1} r_m) J_n(k_{m+1} r_m) - Y_n(k_{m+1} r_m) J_n'(k_{m+1} r_m)]. \quad (5e)$$

The corrected formulas provide the right fields both inside and outside the cylinders, whereas the error affected only the results inside the cylinders, not outside them.

Manuscript received November 15, 1994; revised March 24, 1995.

S. Caorsi is with the Department of Electronics, University of Pavia, Via Abbiategrasso 209, 27100 Pavia, Italy.

M. Pastorino is with the Department of Biophysical and Electronic Engineering, University of Genoa, Via Opera Pia 11A, 16145 Genova, Italy.

IEEE Log Number 9412229.

[1] H. E. Bussey and J. H. Richmond, *IEEE Trans. Antennas Propagat.*, vol. AP-23, pp. 723–725, Sep. 1975.

Lateral Wave Contribution to the Radiation from a Dielectric Half Medium

Reuven Shavit and Eitan Rosen

Abstract— **Two methods are presented for the computation of the radiation at microwave frequencies in a thin dielectric medium from a source located in a dense dielectric medium. One is based on geometrical optics and the other on physical optics. The geometrical optics approach encounters some difficulties in the evaluation of the radiation in the thin dielectric medium near grazing-incidence condition, due to excitation of a lateral wave, which is not taken in consideration by this approach. The physical optics method, which considers the lateral wave contribution approaches this problem successfully and gives a better approximation of the radiated field near grazing. Numerical results, which compare the two methods, and experimental data are offered to validate the theoretical approach.**

I. INTRODUCTION

The interest in the radiation from a dense dielectric medium to a thinner one traces back to Sommerfeld [1], who was the first to evaluate the radiation from horizontal and vertical elementary dipoles embedded in a dielectric half medium. The radiation problem was revisited and investigated in depth by Brekovskikh [2], Banos [3], Wait [4], King and Smith [5], and recently by Chew [6]. The problem was formulated by matching the boundary conditions of the tangential electric and magnetic fields at the interface between the mediums and the Green's function was computed. The far field radiation was computed by using asymptotic techniques like the steepest descent method. If the source is located in the denser medium a lateral wave is excited in addition to the reflected and transmitted waves. Intensive research to investigate the nature of the lateral wave have been conducted by Staiman and Tamir [7], Felsen [8], and King *et al.* [9]. Tamir and Dence [10]–[12] characterized the propagation in forest environments by utilizing ray tracing techniques and the knowledge gained on the lateral wave nature. Their research and the experimental results focused in the 2–200 MHz frequency band. Most of the work published so far considered the radiation field from a horizontal or vertical dipoles in both mediums for radiation angles far from grazing and at relatively low frequencies.

For this reason, an investigation has been initiated in order to evaluate the radiation at grazing angles to the interface in the thin dielectric medium for a horn antenna and at microwave frequencies. The radiating antenna is embedded in the dense dielectric medium and located, relatively close to the interface (Fresnel approximation) [13]. Two methods for the computation will be presented, one based on geometrical optics and the other on physical optics.

The main contribution of this study is to show the importance of the lateral wave to the computation of the radiation at angles near grazing in the thin dielectric medium at microwave frequencies. Banos [3] and others showed its significance, if the observation point is located in the dense dielectric medium and Tamir [11] showed its importance along mixed paths in forest environments. The lateral

Manuscript received May 20, 1993; received January 9, 1995.

R. Shavit is with the Department of Electrical Engineering, Ben-Gurion University of the Negev, Beer-Sheva 84105, Israel.

E. Rosen is with Intel Corp., Haifa, Israel.

IEEE Log Number 9411456.

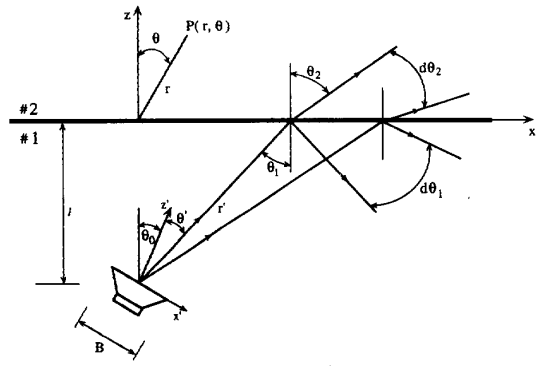

Fig. 1. The basic configuration of the radiating antenna.

wave contribution is absent in the geometrical optics approach and accordingly, it affects the accuracy of the computation giving an edge to the physical optics approach. Experimental results support the theoretical predictions.

II. THEORY

A. Geometrical Optics Approach

The basic configuration is shown in Fig. 1. The radiating antenna is a horn with aperture dimensions $A * B$, embedded in medium 1. The horn is linearly polarized with the electric field x' directed. Medium 1 is denser than medium 2 ($\varepsilon_1 > \varepsilon_2$) and is lossy ($\tan\delta_1 \neq 0$). Without loss of generality, we will assume that medium 2 is free space. The radiating antenna is inclined an angle θ_0 and is located at a distance l from the interface. The center point of the radiating aperture is at the origin in (x', y', z') coordinate system and at $(0, 0, -l)$ in (x, y, z) coordinate system. An incident ray from the antenna making an angle θ_1 (in medium 1) makes an angle θ_2 (in medium 2) undergoing refraction (according to Snell's law).

Throughout the derivation by the geometrical optics approach, it is assumed that the interface is in the Fraunhofer region (far field approximation) of the radiating antenna ($r_0 > \frac{A*B}{\lambda}$). This assumption, will be refined later on as we apply the Fresnel approximation to the physical optics approach. Due to the symmetry of the structure in the xy-plane, the azimuthal radiation pattern of the antenna in medium 2 (free space) for a given θ, remains unchanged compared to the azimuthal radiation pattern when both mediums are free space. Experimental verification proved this assumption to be valid. Accordingly, our interest will be focused only into the elevation radiation pattern in the principal planes x', z' and xz (planes of incidence). In addition, we will assume that the field distribution in the radiating aperture will not be affected by the presence of the interface near it. This assumption has been tested by measuring the VSWR of the radiating antenna with and without medium 1 and no significant change has been detected.

The radiation pattern in medium 2, computed by geometrical optics approach, can be completed in two steps:

1) Computation of the incident electric field at the interface between the two mediums taking in consideration the absorption loss in medium 1.
2) Computation of the transmitted electric field in medium 2 taking in consideration the reflection and refraction at the interface of the incident spherical wave electric field (see Fig. 1).

Given the E-plane radiation pattern, $f_e(\theta')$, of the source antenna, we can compute the radiation pattern of the antenna in medium 2 by geometrical optics approach

$$F(\theta) = f_e(\theta')\frac{2\cos\theta_2}{\cos\theta_1 + n\cos\theta_2}L_b \tag{1}$$

in which $n = \sqrt{\varepsilon_1/\varepsilon_2}\cdot L_b$ represents the absorption loss along a ray trajectory r' (see Fig. 1) and can be approximated (for a low-loss medium) by $L_b = e^{-1/2k_1\tan\delta_1 r'}$ (k_1 is the propagation constant in medium 1).

In (1) the spherical dependence, $\frac{e^{-jk_1 r}}{r}$, of the electric field has been suppressed. It is interesting to note that for $\theta = \theta_2 = \pi/2, F(\theta) = 0$. This result of the geometrical optics approach implies that, at grazing, the electric field is zero.

B. Physical Optics Approach

The computation of the radiation pattern by the physical optics approach is completed in two steps:

1) Computation of the electric field distribution just above the interface at $z = 0^+$ (see Fig. 1).
2) Computation of the radiation pattern from the aperture field distribution on the interface at $z = 0^+$.

The computation of the field distribution at the interface is affected by the lateral wave excitation [2]. Such a contribution is absent in the geometrical optics approach, but is taken in consideration using the physical optics approach. Throughout the computation we assume that medium 1 is low loss and it doesn't affect the field distribution on the radiating antenna. The radiating antenna in medium 1 is a horn with dimensions $A*B$. Upon the computation of the field distribution at the interface we can improve by using the Fresnel approximation. Following a well-known procedure outlined in [13], one can derive the Fresnel zone approximation of the incident θ' component of the electric field, on the interface

$$\begin{aligned} E_i = {} & \frac{1}{B}\sqrt{\frac{\pi}{2\alpha}}(1+\cos\theta') \\ & \times \{C(B_u) - C(B_L) - j[S(B_u) - S(B_L)]\} \\ & \times e^{j\frac{k_1^2\sin^2\theta'}{4\alpha}} L_b \frac{e^{-jk_1 r'}}{r'} \end{aligned} \tag{2}$$

where

$$\alpha = \frac{k_0}{2\rho_e} + \frac{k_1\cos^2\theta'}{2r'} \tag{3}$$

$$B_L = -\sqrt{\frac{2\alpha}{\pi}}\left(\frac{B}{2} + \frac{k_1\sin\theta'}{2\alpha}\right) \tag{4}$$

$$B_u = \sqrt{\frac{2\alpha}{\pi}}\left(\frac{B}{2} - \frac{k_1\sin\theta'}{2\alpha}\right). \tag{5}$$

L_b denotes the absorption loss along a ray trajectory in medium 1, ρ_e is the distance from the horn phase center to its aperture and $C(x), S(x)$ are Fresnel integrals [13]. To obtain the field distribution above the interface, we have to impose boundary conditions upon the tangential electric and magnetic fields at $z = 0$.

Fig. 2 shows all the contributions to the total electric field (θ' component) at the observation point $P(r', \theta')$ in medium 1 in the principal plane x', z'. These are E_i, E_r, and E_L the direct, reflected and lateral waves, respectively. If we denote by $\theta_c = \sin^{-1}(1/n)$ the critical angle (total reflection angle at the interface), the lateral wave propagates only for angles $\theta_1 \geq \theta_c$. Thus, for radiation angles $\theta_1 < \theta_c$ only the direct (E_i) and reflected waves (E_r) contribute

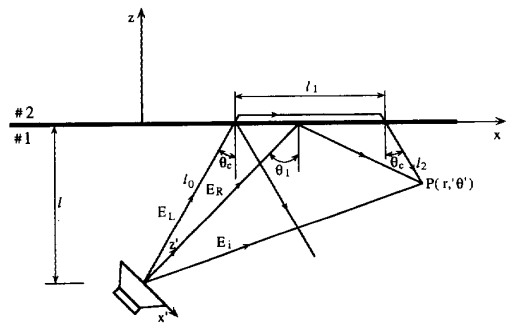

Fig. 2. The electric field contributions to an observation point P in medium 1.

to the total field at $P(r', \theta')$, while for radiation angles $\theta_1 \geq \theta_c$ an additional contribution exists due to the lateral wave, E_L, excitation. Brekovskikh [2], Staiman *et al.* [7], Felsen [8] and King *et al.* [9] investigated, thoroughly the nature of the lateral wave. This wave is excited only if the radiating antenna is located in the denser medium. Moreover, once it is excited, it can be characterized by an up-going ray (l_0) at the critical angle, a parallel ray (l_1) to the interface in medium 2, and a down-going ray (l_2) at the critical angle as shown in Fig. 2.

The continuity of the tangential electric and magnetic fields determines the boundary conditions to be satisfied at $z = 0^+$ in the principal plane x, z. Since the reflection coefficient, R, is accounted for the continuity of the tangential magnetic field, we may have to impose only continuity of the tangential electric field, E_t, at $z = 0^+$. Thus

$$E_t = \begin{cases} E_i(1 - R)\cos\theta_1 & \theta_1 < \theta_c \\ E_i(1 - R)\cos\theta_1 - E_L\cos\theta_c & \theta_1 = \theta_c \\ -E_L\cos\theta_c & \theta_1 > \theta_c. \end{cases} \tag{6}$$

In the domain $\theta_1 < \theta_c$ the reflection coefficient R is the reflection coefficient [14] for an incident planar wave with the electric field linearly polarized in the plane of incidence x', z', which is the geometrical optics approximation. In the transition domain $\theta_1 \approx \theta_c$, however, this approximation is not accurate due to the excitation of the lateral wave and we need a better approximation. Brekovskikh [2] computed such an approximation for the reflection coefficient, R in the vicinity of the critical angle given by

$$R = 1 - \frac{4ne^{-j\pi/8}}{\Gamma(1/4)(k_1 r_1/2)^{1/4}}\sqrt{\frac{\pi}{\sin 2\theta_c}} \times \left[1 - j\frac{\eta^2}{2} + \frac{1}{2!}\left(\frac{\eta^2}{2}\right)^2 + j\frac{7}{3!5}\left(\frac{\eta^2}{2}\right)^3 \cdots\right] \tag{7}$$

where

$$\Gamma(1/4) = 3.6256 \quad \eta = \sqrt{2k_1 r_1}\sin\frac{\theta_1 - \theta_c}{2} \tag{8}$$

and r_1 is the distance from the "virtual" source to the observation point $P(r', \theta')$. If the observation point is on the interface $r_1 = r'$, close scrutiny into (7) reveals that $R \approx 1$ at the critical angle, as expected. The lateral wave, E_L generated by an elementary vertical dipole in a dielectric half medium has been computed by Brekovskikh [2]. This expression is valid for the entire range of the lateral wave's existence $\theta_1 \geq \theta_c$. If we multiply this expression by the incident electric field, $E_i(\theta_c, l_0)$ at the critical angle as given by (2), we obtain the lateral wave generated in the principal plane x, z in medium 2, along the interface at $z = 0^+$. Such an exercise yields

$$E_L = -E_i(\theta_c, l_0)\frac{2jn^2}{k_0(n^2 - 1)}\frac{l_0}{\sqrt{\rho}l_1^{3/2}}e^{-jk_0 l_1}F(\eta) \tag{9}$$

in which ρ is the radial distance in cylindrical coordinates (ρ, ϕ, z) and $F(\eta)$ is the Fresnel integral [13] with the argument η given by (8). The asymptotic expansion of $F(\eta)$, useful in the range $\theta_1 \approx \theta_c$, in powers of η can be found in [2] and is reproduced here

$$F(\eta) = \sqrt{\pi}e^{-j3\pi/8}\eta^{3/2} \times \left\{\frac{4}{\Gamma(1/4)}\left[1 - j\frac{3\eta^2}{2} - \frac{7}{2}\left(\frac{\eta^2}{2}\right)^2 + \cdots\right] - \sqrt{\frac{2(1-j)\eta}{\Gamma(3/4)}}\left[1 - j\frac{5}{3}\left(\frac{\eta^2}{2}\right) - \frac{9}{2*3}\left(\frac{\eta^2}{2}\right)^2 + \cdots\right]\right\}. \tag{10}$$

It is interesting to note that as $\theta_1 \rightarrow \theta_c$ the amplitude of the lateral wave does not vanish, as it would seem at first glance. In the vicinity of the critical angle, the lateral wave amplitude, E_L is highly dependent on the ratio of $F(\eta)$ and $l_1^{3/2}$. All other quantities in (9) behave monotonic; however, this ratio is finite at the limit $\theta_1 \rightarrow \theta_c$, as one can observe by studying Fig. 2 and (10). In the range $\theta_1 > \theta_c$, $F(\eta)$ as given by (10) is nonconvergent and we need the asymptotic expansion of $F(\eta)$ in powers of $1/\eta^2$ [2]

$$F(\eta) = 1 - \frac{3*5*7*9}{2*4(8\eta^2)^2} + \cdots - \frac{15j}{16\eta^2}\left(1 - \frac{7*9*11*13}{4*6(8\eta^2)^2} + \cdots\right). \tag{11}$$

The lateral wave significance is in the fact that it extends the existence of the electric field in medium 2 beyond the critical angle point. This observation is in contrast to the geometrical optics approach, which predicts zero field beyond the critical angle point. Inspection of (9) reveals that beyond the critical angle point the field distribution decays as $0(\rho^{-2})$ and it has a progressive phase along the interface.

The tangential electric field distribution on the interface, E_t, can be viewed as the source of the radiated field in medium 2 in the principal plane x, z. Standard procedure [13] transforms the electric field distribution into equivalent magnetic current distribution on the interface. Given the equivalent sources, one can show [13] that the radiation pattern in the x, z plane is given by

$$f(\theta) = \int_{S_a} E_t(x')e^{jk_0 x'\sin\theta}\,dx' \tag{12}$$

where S_a is the aperture dimension on the interface. One can notice that the radiation pattern in medium 2 is actually the Fourier transform of the field distribution on the interface. Accordingly, a standard FFT routine can be applied to compute (12) in a fast and efficient way.

III. RESULTS

A test module made of plywood and internally plated with absorbing materials (except of the radiating aperture) was constructed. The module was filled with silica ($\varepsilon_r = 2.1, \tan\delta = 50 \cdot 10^{-4}$ to simulate the radiation conditions from a half dielectric medium. The module's dimensions were 1.5 m (L), 0.6 m (W), and 0.7 m (H). The transmitting antenna was located 30 cm beneath the silica

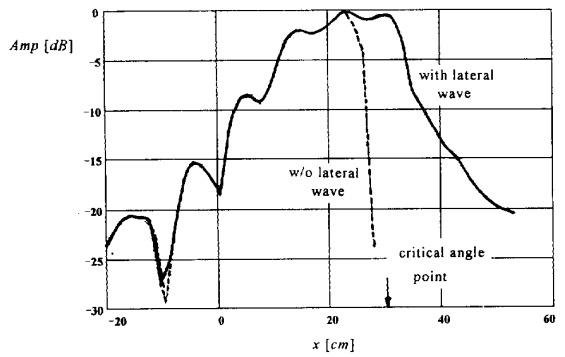

Fig. 3. The computed, E_t, field distribution on the interface ($\theta_0 = 40$ degrees, $l = 30$ cm, $f = 5.7$ GHz).

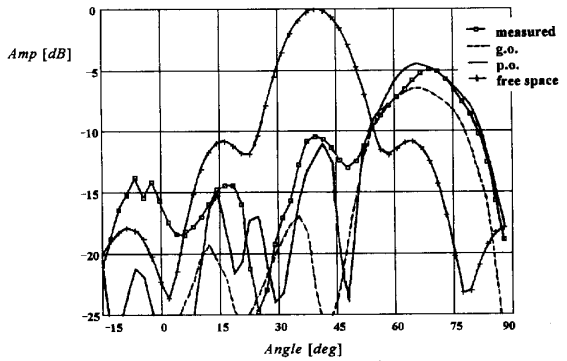

Fig. 4. Measured and computed radiation patterns ($\theta_0 = 40$ degrees, $l = 30$ cm, $f = 5.7$ GHz).

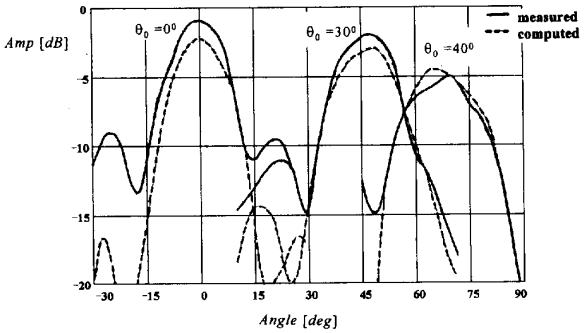

5. Radiation patterns for different θ_0 inclination angles ($l = 30$ cm, $f = 5.7$ GHz).

and the air interface. The module was placed on a azimuth-over-elevation positioner and rotated to measure azimuth and elevation patterns. Both transmitting and receiving antennas were chosen to be standard horns with dimensions $17 * 20$ cm and $\rho_e = 35$ cm. The distance between the receiving and transmitting antennas was 12 m to fulfill the far field criterion for the operating frequency (5.7 GHz). The system was calibrated with the transmitting and receiving antennas in free space without the silica.

Fig. 3 shows the dependence of the computed, E_t, tangential electric field distribution on the interface as a function of the coordinate x. The inclination angle, θ_0 of the radiating antenna was 40 degrees. As one can notice, the tangential electric field has shallow nulls and sidelobes, since the interface is located in the Fresnel region of the radiating antenna. Moreover, the amplitude of the electric field extends beyond the critical angle point due to the lateral wave contribution. The decay of the field beyond this point is $0(x^{-2})$. In comparison is shown the field distribution without the lateral wave contribution. One can observe that without the lateral wave contribution the field amplitude drops rapidly close to the critical angle point. The fine structure of the field distribution near the critical angle determines solely the radiation pattern for angles near grazing and has a cardinal effect upon the radiated field accuracy.

Fig. 4 shows the computed (g.o. and p.o. approaches) and measured patterns in medium 2 with the geometry parameters $\theta_0 = 40$ degrees, $l = 30$ cm. For comparison, the radiation pattern of the transmitting horn (oriented at 40 degrees) in free space is plotted. The system is calibrated to the received signal in free space. The peak location of the computed (by both methods) and measured patterns differ slightly and agrees well with Snell's law [14]; however, the slope near grazing is different. The descend of the radiation pattern computed through physical optics approach with the lateral wave contribution, shows a better agreement to the measured data. In addition, one can observe a significant beam broadening of the pattern through the silica compared to that in free space. This beam broadening can be attributed to the refraction at the interface. The agreement between the computed and measured patterns in the region around 0 degrees is less satisfactory. This result may be caused by the diffraction from the edges of the test module (finite in length). The computation through physical optics considers an infinite interface length (x-axis in Fig. 1) without any diffraction effects. This diffraction effect may be negligible in the main beam as shown in Fig. 4, but significant compared to the sidelobes.

Fig. 5 shows the dependence of the radiation pattern on the inclination angle, θ_0, of the radiating antenna in the silica. The theoretical patterns have been computed with the physical optics approach. For θ_0 angles close to the critical angle, θ_c, we can identify three observations: the slope of the radiated field near grazing is constant, the peak location of the main beam moves toward grazing according to Snell's law, and the level of the main beam peak decreases due to an increase in the reflection coefficient from the interface. The difference in the sidelobe levels for the case $\theta_0 = 0$ degrees between the measured and theoretical computations may be caused by parasitic diffraction from the back and sidewalls of the test module.

IV. CONCLUSION

The purpose of this study was to determine the radiation pattern in a thin dielectric medium from an antenna embedded in a dense dielectric medium. Two methods for computation were presented and compared to experimental data. The physical optics approach proved to be more accurate than the geometrical optics approach for radiation angles close to grazing. The lateral wave contribution to the field distribution beyond the point of total reflection proved to be significant for near grazing radiation angles. The theory has been tested experimentally and the agreement has been found to be satisfactory.

ACKNOWLEDGMENT

The authors wish to express their appreciation to S. Raz of the Technion-Israel Institute of Technology, Haifa, for his help and stimulating discussions on the subject, and to R. Osirof and his group for the fabrication and design of the test module for the experiments.

REFERENCES

[1] A. Sommerfeld, *Partial Differential Equations in Physics*. New York: Academic, 1949, pp. 246–261.

[2] L. M. Brekovskikh, *Waves in Layered Media*. New York: Academic, 1980, pp. 255–273.

[3] A. Banos, *Dipole Radiation in the Presence of a Conducting Half Space*. New York: Pergamon, 1966, pp. 195–235.

[4] J. R. Wait, *Electromagnetic Waves in Stratified Media*. New York: Pergamon, 1970.

[5] R. W. P. King and G. S. Smith, *Antennas in Matter: Fundamentals, Theory and Applications*. Cambridge, MA: MIT Press, 1981.

[6] W. C. Chew, *Waves and Fields in Inhomogeneous Media*. New York: Van-Nostrand, 1990.

[7] D. Staiman and T. Tamir, "The nature and optimization of the ground (lateral) wave excited by submerged antennas," *Proc. IEE*, vol. 113, Aug. 1966.

[8] L. B. Felsen, *Electromagnetic Wave Theory*, J. Brown, Ed. New York: Pergamon, 1967, pp. 11–43.

[9] R. W. P King, M. Owens, and T. T. Wu, *Lateral Electromagnetic Waves*. New York: Springer-Verlag, 1992.

[10] T. Tamir, "On radio wave propagation in forest environments," *IEEE Trans. Antennas Propagat.*, vol. AP-15, no. 6, Nov. 1967.

[11] ——, "Radio wave propagation along mixed paths in forest environments," *IEEE Trans. Antennas and Propagat.*, vol. AP-25, no. 4, July 1977.

[12] D. Dence and T. Tamir, "Radio loss of lateral waves in forest environments," *Radio Sci.*, vol. 4, no. 4, Apr. 1969.

[13] C. A. Balanis, *Antenna Theory*. New York: Harper & Row, ch. 12, pp. 532–545, 1981.

[14] E. C. Jordan and K. G. Balmain, *Electromagnetic Waves and Radiating Systems*. Englewood Cliffs, NJ: Prentice-Hall, ch. 5, pp. 129–147, 1968.